buildings

MDPI

Article

The Effect of Enclosure Layout on Wind Environment in Chinese Classic Landscape Gardens: A Case Study of Beijing's Summer Palace Ruins Garden

Zefa Wang [1,2], Min Wang [1,*], Yaolong Wang [1], Tiantian Huang [3], Jing Chen [4,5] and Tingfeng Liu [1,*]

[1] School of Architecture, Tianjin University, Tianjin 300072, China; zefawang@qztc.edu.cn (Z.W.); wangyaolong@tju.edu.cn (Y.W.)
[2] School of Resources and Environmental Sciences, Quanzhou Normal University, Quanzhou 362000, China
[3] School of Fine Arts and Design, Quanzhou Normal University, Quanzhou 362000, China; huangtiantian@stumail.qztc.edu.cn
[4] Institute of Geography, Fujian Normal University, Fuzhou 350007, China; chenjing87@fjnu.edu.cn
[5] School of Geographical Sciences, Fujian Normal University, Fuzhou 350007, China
* Correspondence: wangmin840025@hotmail.com (M.W.); tfliu1967@tju.edu.cn (T.L.)

Abstract: The design of the enclosure layout is crucial in establishing a comfortable wind environment in Chinese classic landscape gardens. The Ruins Park of the Old Summer Palace exemplifies the mountain construction techniques used in classical Chinese flat gardens, with a diverse and illustrative spatial layout of the hills. In this study, we focused on the earthen hill space of the Old Palace in the Summer Palace Ruins Park. We compared and analyzed the effects of different enclosure layouts of earthen hill spaces on the summer monsoon wind environment. This was achieved via on-site measurements and simulations using computational fluid dynamics (CFD). The results show the following: (1) The direction index of the enclosure layout of the earthen hill space affects wind speed, comfort, and ventilation. Increasing the index reduces speed and comfort but improves ventilation. (2) Increasing the density index of the enclosure layout of the earthen hill space leads to a decrease in wind speed and wind comfort and improved ventilation. (3) Conversely, increasing the area index of the enclosure layout of the earthen hill space results in an increase in wind speed, which can result in better wind comfort but can also lead to poor ventilation. Overall, the results suggest that careful consideration should be given to the enclosure layout of landscape gardens to ensure optimal wind conditions within the space.

Keywords: Beijing; Old Summer Palace Ruins Park; earthen hill space; environmental quality assessment of the enclosure layout; wind comfort

Citation: Wang, Z.; Wang, M.; Wang, Y.; Huang, T.; Chen, J.; Liu, T. The Effect of Enclosure Layout on Wind Environment in Chinese Classic Landscape Gardens: A Case Study of Beijing's Summer Palace Ruins Garden. *Buildings* **2024**, *14*, 280. https://doi.org/10.3390/buildings14010280

Academic Editor: Ricardo M. S. F. Almeida

Received: 16 November 2023
Revised: 18 December 2023
Accepted: 16 January 2024
Published: 19 January 2024

1. Introduction

Chinese classical landscape gardens are designed on the basis of the ancient enclosure theory, namely the Feng Shui theory, which was developed during the Shang and Zhou Dynasties in China and developed further during the Tang and Song Dynasties. The ancient theory of enclosure consists of two phases: the phase of the shape and the compass. The shape phase emphasizes the use of natural terrain, the appropriate selection of locations, and strategic constructions and graves [1]. This approach is considered to be the norm in enclosure theory, and the layout follows the principle of selecting more solar- and heat-generating sites in summer and prohibiting strong and cold winds in winter. The approach gradually resulted in the formation of an enclosure model of four surrounding elements in terms of hills or mountains, namely the east Qinglong, the west White Tiger, the south Vermillion Phoenixes, and the north Black Turtles [2], as shown in Figure 1a. Each of the four elements played a major role in forming an ideal enclosure for a classical garden with an acceptable wind environment in the central human living and working space.

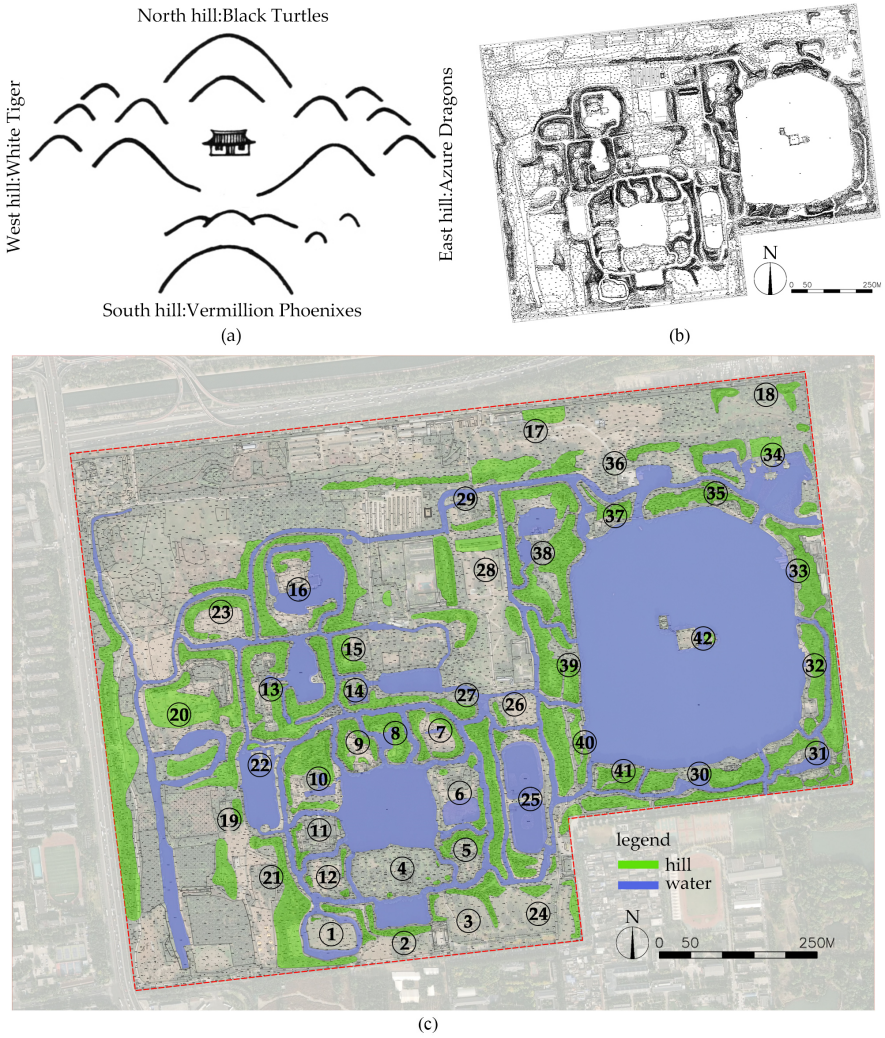

Figure 1. (**a**) Enclosure layout mode of earthen hill space. (**b**) Measured topographic map of Old Summer Palace Ruins Park in 2016. (**c**) Spatial distribution map of 42 earthen hills in the Old Summer Palace Ruins Park.

At present, there are few scientific investigations into the wind environment based on the ancient enclosure theory with respect to classic gardens; rather, they usually concentrate on traditional villages, courtyards, architecture, natural mountains, and other related topics. For example, CFD was employed by Li Tang et al. to examine the enclosure model of a village, and the results of the study revealed that its layout is suitable for the local environment [3]. Zhao Z. et al. investigated the enclosure theory employed in ancient China and assessed the effectiveness of the enclosure design in the Bailudong Academy complex using CFD simulation techniques [4]. Similarly, Guo et al. used Prince Kung's Mansion in Beijing as an example to demonstrate that the enclosure layout can improve the courtyard wind environment in the summer [5]. Wang K. et al. implemented CFD technology in order to simulate wind fields with different mountain terrain slopes, shapes, and patterns. Subsequently, they proposed wind-sensing planning strategies based on the results of their research [6]. Zhou Z. et al. conducted a study to compare the wind and heat environment of four traditional village mountain patterns in Jiangxi Province, and the findings of the analysis confirmed the validity of the principle of mountains at the back and water at the front [7]. However, the impact of the enclosure theory on spatial wind environments containing artificial hills has not been extensively studied, and there is a need for further investigation. Therefore, it is necessary to investigate the spatial wind environment of artificial hills in the arrangement of enclosure elements.

CFD simulation has been widely applied to study the physical environments of various places, ranging from villages to neighborhoods and from buildings to courtyards, both indoors and outdoors. Xiong Y. et al. conducted a study to examine the correlation between Jiangnan traditional villages and microclimate comfort. The results indicated that the sites of traditional villages were chosen based on the local conditions, taking advantage of the nearby landscape to create a more comfortable and pleasant living environment for the villagers [8]. Wang Z. et al. conducted a measured analysis and CFD simulations to examine the influence of various types of village entrance space on the wind environment in Jinxi County, Eastern Jiangxi Province [9]. Ai Z. T. and Mak C. M. conducted a CFD simulation to demonstrate that the flow field inside an urban street canyon can be accurately predicted using a T-shaped computational domain, which connects the street canyon to the free flow layer above it [10]. Gan S. et al. conducted an evaluation of the potential of wind energy generated from through-building openings under the influence of twisted wind flows [11]. Almhafdy et al. conducted a CFD simulation to assess the impact of aspect ratio and cantilever roofs on courtyard wind speeds and thermal comfort, and the results confirmed the significance of these factors [12]. Conceicão et al. conducted a CFD simulation to compare the air distribution index (ADI) of a classroom containing six people and twelve people, thus providing a benchmark for the placement of air terminal devices [13]. Utilizing CFD simulation, Hong B. et al. evaluated the effect of exterior trees on the diffusion of PM1.0, PM2.5, and PM10 inside a naturally ventilated auditorium [14]. Zhao Y. et al. conducted a study to assess the potential of trees in ameliorating the microclimate and reducing the urban heat island (UHI) effect via the use of an ENVI-met model of a courtyard in North China [15]. It has been established that CFD simulations can accurately assess the connections between villages, communities, buildings, and courtyard wind environments. As such, we utilized CFD simulation to explore the spatial wind environment of different types of enclosure layouts in earthen hills.

We took the earthen hill space of the Old Summer Palace Ruins Park as the research object and divided the space into types according to the distribution of the enclosure layout of the earthen hill space. The focus was on exploring the impact of different enclosure layout types of the earthen hill space on the outdoor wind environment. Initial experiments indicated that ventilation during the summer season is essential for outdoor activities in the earthen hill space. Consequently, CFD simulation and on-site measurement of the earthen hill space in the Old Summer Palace Ruins Park were conducted during the summer. Investigation of the spatial wind environment during winter in the earthen hill space is also significant for the analysis of the layout of the enclosure. This is an aspect that will be looked into in the future.

By combining CFD simulation and summer field measurements, we aimed to explore the effect of the enclosure layout on the spatial wind environment of an earthen hill, thereby verifying the ecological design of ancient China in the enclosure layout of the earthen hill.

2. Research Object and Methods

2.1. Research Object: Enclosure Layout of Earthen Hill Space in Old Summer Palace Ruins Park

2.1.1. Overview of Earthen Hill Space in Old Summer Palace Ruins Park

The Old Summer Palace Ruins Park is located in Haiding District, Beijing, China, between 116°16′–116°19′ East and 39°59′–40°0′ North. It is characterized by a warm temperate semi-humid and semi-arid monsoon climate, and it was previously the site of the imperial garden of the Old Summer Palace during the Qing Dynasty.

The Old Summer Palace, bestowed by Emperor Kangxi of the Qing Dynasty, reached its peak with extensive expansion during the Yongzheng and Qianlong Dynasties. It is renowned as the "Garden of Ten Thousand Gardens" and is a masterpiece in respect of the techniques of building mountains and managing water in Chinese classical flat gardens [16]. In 1860, it was ravaged by disaster and war, which erased its buildings and vegetation, yet the structures of its mountains and rivers remain largely intact, particularly the earthen hills. The terrain and landforms of the earthen hills located in the Houhu District, Beiyuan

District, and Fuhai District have been restored and are now relatively complete. In 1988, the Old Summer Palace Ruins were designated as a National Key Cultural Relics Protection Unit, and the Ruins Park was opened to the public.

The 2016 CAD topographic map of the Old Summer Palace Ruins Park (Figure 1b) shows that the entire earthen hill space in the park can be divided into 42 relatively independent earthen hill spaces (Figure 1c), with the main earthen hill system being separated and enclosed, and the auxiliary water system also being separated and enclosed. Each earthen hill space contains earthen hills distributed in four directions, and the layout of the earthen hills in each space follows the ancient enclosure theory.

2.1.2. Enclosure Layout Index in the Earthen Hill Space of the Old Summer Palace Ruins Park

Earthen hill enclosure layout indices, which have an impact on the spatial wind environment, can be divided into two categories: planar indices and facade indices. Direction, density, and area index are the three most important planar indices. To evaluate the direction, density, and area index of the earthen hill enclosure layout, a quantitative equation was established after a thorough review of related literature and field research.

(1) Direction Index of the Enclosure Layout in an Earthen Hill Space

The direction index of the enclosure layout of an earthen hill is a measure of the extent of the azimuthal enclosure of the earthen hill, and it is computed by dividing the number of directions of the earthen hill by the total number of directions in the four cardinal directions, i.e., east, south, west, and north (Equation (1); Figure 2a).

$$S = N \tag{1}$$

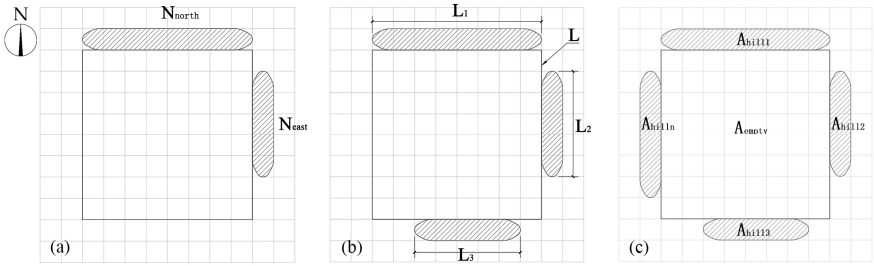

Figure 2. (**a**) Schematic diagram of direction index for the enclosure layout in an earthen hill space. (**b**) Schematic diagram of density index for the enclosure layout in an earthen hill space. (**c**) Schematic diagram of area index for the enclosure layout in an earthen hill space.

In this index, the S-value of the enclosure layout of an earthen hill is denoted by N, which is the sum of the number of directions in which the hill exists—east, south, west, and north—with a maximum value of 4, implying that the earthen hill exists in all four directions, namely east, south, west, and north.

(2) Density Index of the Enclosure Layout in an Earthen Hill Space

The density index of the enclosure layout in the earthen hill space is calculated by dividing the total length of the earthen hill facades around the earthen hill space by the total circumference of the earthen hill space (Equation (2); Figure 2b). This index is used to measure the density of the spatial arrangement of the enclosures in the earthen hill.

$$S = \frac{C}{L} \tag{2}$$

The density ratio of the enclosure layout in the earthen hill space, S, is determined by the total circumference, C, of the earthen hill facade around the earthen hill space, which is the sum of all the individual lengths, $L_1 + L_2 + ... + L_n$. The higher the layout density of the enclosures in the earthen hill space, the greater the value of S.

(3) Area Index of the Enclosure Layout in an Earthen Hill Space

The area index of the enclosure layout of an earthen hill is the ratio of the spatial area of the earthen hill to the area of its surrounding earthen hill, as shown in Equation (3) and Figure 2c. This index is used to measure the layout area of the enclosures in the earthen hill in this study.

$$S = \frac{A_{empty}}{A_{hill}} \quad (3)$$

The ratio of the layout area of the enclosures in the earthen hill space, S, is dependent on the size of the earthen hill space, A_{empty}, and the land area of the surrounding earthen hill, A_{hill}. The larger the spatial area of the earthen hill and the smaller the land area of the surrounding earthen hill, the greater the value of S, resulting in a more open space of the earthen hill.

Utilizing AutoCAD v.2010 software, 42 earthen hill spaces in the Old Summer Palace Ruins Park were separately extracted (Figure 3). Subsequently, the direction, spatial perimeter, total length of the surrounding earthen hill, spatial area of the earthen hill, and area of the surrounding earthen hill were statistically analyzed for each earthen hill space. The direction, density, and area index equations were then utilized to obtain the numerical statistical table for the enclosure layout direction, density, and area in the 42 earthen hill spaces of the Old Summer Palace Ruins Park (Table 1).

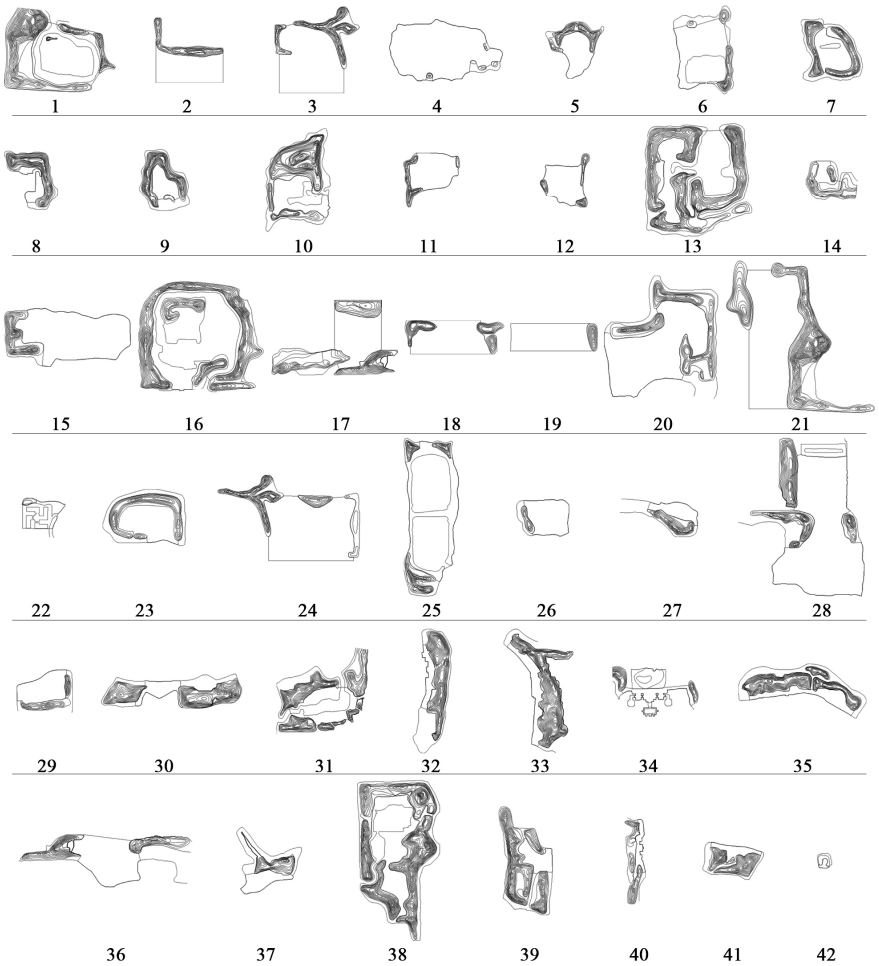

Figure 3. Topographic maps of 42 earthen hill spaces in the Old Summer Palace Ruins Park.

Table 1. Statistical table for the enclosure layout direction, density, and area index of 42 earthen hills spaces in the Old Summer Palace Ruins Park.

Figure No.	Direction Index	Density Index	Area Index	Figure No.	Direction Index	Density Index	Area Index
1	4	0.886	1.034	22	1	0.119	14.406
2	1	0.351	2.914	23	4	0.761	1.241
3	3	0.482	3.174	24	3	0.563	2.967
4	2	0.128	42.291	25	2	0.284	6.155
5	3	0.452	1.710	26	1	0.210	8.120
6	2	0.288	6.573	27	1	0.405	1.134
7	4	0.957	0.880	28	3	0.419	2.907
8	3	0.410	0.415	29	2	0.478	2.514
9	4	0.895	0.579	30	2	0.262	0.306
10	4	0.781	0.694	31	4	0.835	0.782
11	2	0.388	4.566	32	3	0.471	0.271
12	2	0.389	5.608	33	2	0.519	0.378
13	4	0.953	0.833	34	3	0.186	0.617
14	3	0.758	0.613	35	2	0.516	0.476
15	1	0.211	5.111	36	2	0.264	1.714
16	4	0.893	1.454	37	1	0.301	1.021
17	2	0.606	0.700	38	4	0.981	0.637
18	2	0.391	2.772	39	3	0.675	0.250
19	1	0.140	9.434	40	2	0.535	0.435
20	2	0.615	2.036	41	3	0.548	0.432
21	3	0.617	1.272	42	3	0.607	0.751

Note: Figure 1 is linked to the first topographic map in Figure 3, and so on.

2.2. Contrastive Research Method

We focused on 42 earthen hill spaces in the Old Summer Palace Ruins Park, all of which adhere to the enclosure layout and have different directions, densities, and area indices. Via a comparative analysis of the summer monsoon environment, it can be concluded that the direction, density, and area index of the enclosure layout of earthen hill spaces have an effect on the summer ventilation performance of such spaces.

To compare the different indices of the enclosure layout in an earthen hill space, SketchUp v.2021 software was applied to model 42 earthen hill spaces in the Old Summer Palace Ruins Park, omitting elements such as architecture, plants, and water, and to analyze the relationship between the enclosure layout in an earthen hill and summer ventilation performance. The models were then imported into PHOENICS v.2016 software for CFD simulation calculations.

2.3. Research Framework

We examined the influence of various enclosure layout indices on the outdoor wind environment by analyzing three indices, i.e., direction, density, and area, of 42 earthen hill spaces in the Old Summer Palace Ruins Park. To ascertain the accuracy of the CFD simulation, a single earthen hill space from the 42 earthen hill spaces in the Old Summer Palace Ruins Park was chosen to compare the measured wind speed values with the CFD simulation wind speed. Autocad v.2010 software was employed to draw topographic maps of the 42 earthen hill spaces in the Old Summer Palace Ruins Park and the direction, density, and area indices of these spaces was calculated. Subsequently, CFD simulations were performed on all 42 earthen hill spaces using PHOENICS v.2016 software in order to compare and analyze the influence of direction, density, and area indices on the outdoor wind environment and to draw research conclusions. The research framework is illustrated in Figure 4.

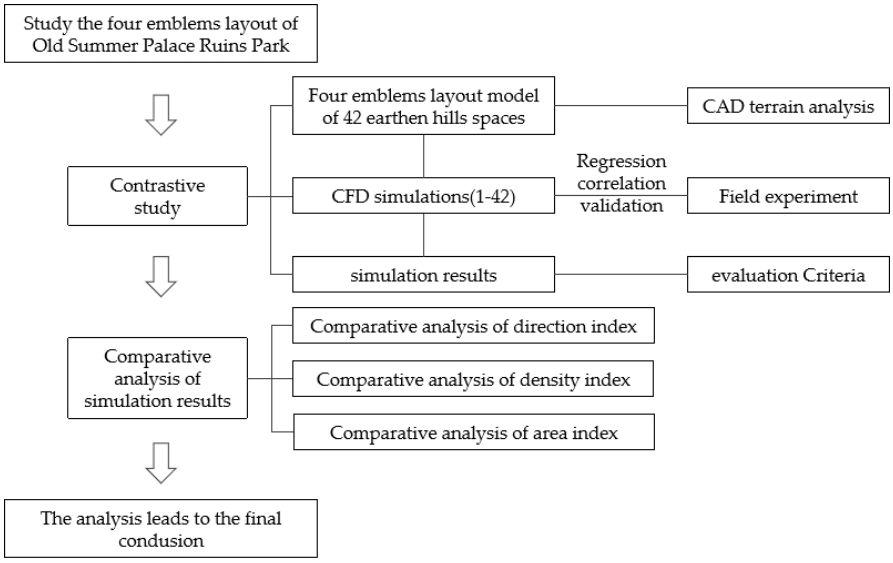

Figure 4. Research framework.

2.4. Evaluation Methods and CFD Simulation

2.4.1. Wind Environment Evaluation Methods in Summer

We focused on the influence of the enclosure layout in the earthen hill space of the Old Summer Palace Ruins Park on the summer monsoon environment. In accordance with the Chinese Green Building Evaluation System and prior studies, evaluation criteria for the summer monsoon environment were established. According to the "Green Building Evaluation Standards" (GB/T 50378-2019), under typical summer wind speed and direction conditions, there should be no vortices or windless areas in the human activity area of the site; more than 50% of the outdoor windows should be openable, and the wind pressure difference between the indoor and outdoor surfaces should be greater than 0.5 Pa [17]. Murakami and Morikawa, as well as Hua Zhang and Tan Luwei, identified three wind speed zones: the low wind speed zone, with wind speeds below 1.0 m/s; the comfortable wind speed zone, with wind speeds between 1.0 m/s and 2.9 m/s; and the strong wind zone, with wind speeds exceeding 2.9 m/s [18–20]. According to the "Green Building Evaluation Standards" (GB/T 50378-2019) and previous research experience, the wind speed data at a distance of 1.5 m from the ground were selected as the wind environment evaluation values.

2.4.2. Details of Wind Environment Experiment and Simulations

(1) Measured Points Selection

In order to better understand the typical division of the horizontal flow field in the earthen hill space of the Old Summer Palace Ruins Park and accurately determine the location of the measured points of the summer wind environment in the horizontal flow field, CFD was used to simulate the wind environment in the earthen hill space case site (Xinghua Chunguan). Nine representative wind speed detection points A (north), B (northwest), C (west), D (southwest), E (south), F (southeast), G (east), H (northeast), and I (center) were selected based on the different regions formed by the summer natural wind after encountering the earthen hill space of Xinghua Chunguan, and the flow field attributes (windward area, angular flow area, flow passage area, vortex area, and wind shadow area) of each point were determined (Figure 5a).

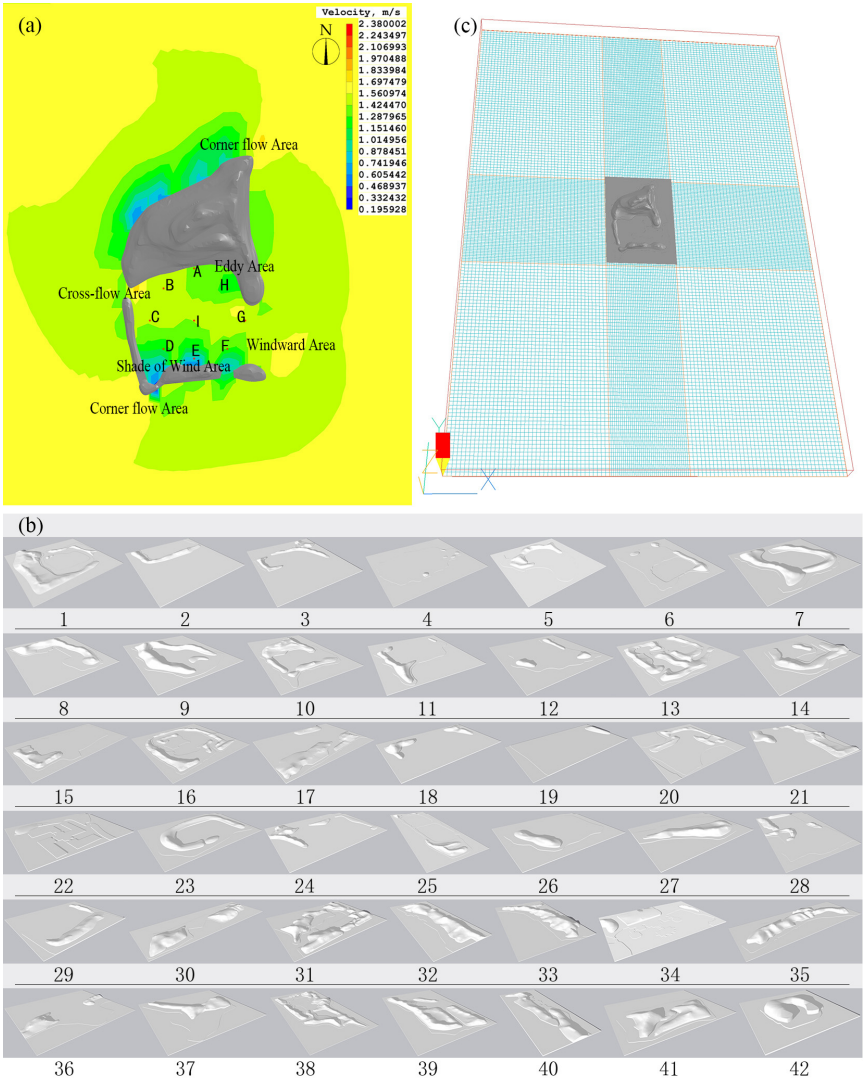

Figure 5. (**a**) Distribution map of wind speed measurement points. (**b**) PHOENICS mesh settings. (**c**) Spatial model of 42 earthen hills in the Old Summer Palace Ruins Park.

(2) Onsite Experiment Method

On 14 September 2022, a simultaneous fixed-point observation was conducted in the earthen hill space of the Xinghua Spring Pavilion in the Old Summer Palace Ruins Park, using the NK5500LINK wind speed meteorological instrument (Kestrel Meters, Boothwyn, PA, USA). Nine measurement points (A–I) were established between 10:00 a.m. and 5:00 p.m. to assess the wind environment and verify the coupling between measured and simulated wind speed values. Subsequently, the detection points for wind environment simulation scenarios were arranged accordingly. Using a tripod-mounted anemometer, wind speed data were collected at nine measurement points, with the anemometer inlet located 1.5 m above the ground. Data were obtained every hour, with the average wind speed within one minute taken as the data value. From 10 a.m. to 5 p.m., a total of 1296 effective wind speed data sets were collected. The collected data were used to calculate the average wind speed for each time period, allowing for comparison and analysis of the wind environment conditions of different measurement points in the earthen hill space. The accuracy of the NK500LNK wind speed meteorological instrument was ±3%.

(3) 3D Model Construction

Based on the CAD topographic maps of 42 earthen hill spatial scenes in the Old Summer Palace Ruins Park, a 3D model for outdoor wind field calculation was established

using SketchUp software after an appropriate simplification and rounding process without affecting the calculation results (Table 2; Figure 5b). This model was then converted into STL format and imported into PHOENICS software for wind environment simulation, yielding wind environment simulation results at a height of 1.5 m (Z = 1.5 m) from the ground for pedestrians.

Table 2. Simplified values of 42 spatial scenes of earthen hills in the Old Summer Palace Ruins Park.

Figure No.	Dimension (m)	Figure No.	Dimension (m)	Figure No.	Dimension (m)
1	250 × 210 × 10.2	15	280 × 140 × 6.7	29	130 × 100 × 4.2
2	170 × 170 × 7.2	16	280 × 270 × 7.2	30	300 × 100 × 9.7
3	190 × 210 × 6.7	17	270 × 190 × 8.2	31	210 × 160 × 8.7
4	250 × 200 × 3.7	18	220 × 130 × 7.7	32	90 × 190 × 8.7
5	140 × 140 × 5.7	19	200 × 110 × 6.2	33	160 × 250 × 11.2
6	160 × 200 × 6.2	20	250 × 270 × 6.7	34	180 × 120 × 7.2
7	150 × 140 × 6.7	21	230 × 310 × 10.2	35	280 × 110 × 9.7
8	130 × 130 × 7.7	22	100 × 70 × 1.7	36	250 × 190 × 8.2
9	120 × 140 × 7.7	23	190 × 130 × 6.7	37	150 × 140 × 8.2
10	160 × 240 × 12.7	24	250 × 180 × 6.7	38	210 × 380 × 11.2
11	140 × 140 × 6.2	25	150 × 370 × 6.2	39	140 × 230 × 6.7
12	140 × 150 × 5.7	26	130 × 100 × 5.2	40	70 × 170 × 5.2
13	250 × 260 × 9.2	27	120 × 90 × 6.2	41	140 × 110 × 8.2
14	110 × 100 × 4.7	28	240 × 380 × 10.2	42	50 × 50 × 4.7

Note: Each dimension in the table represents the length, width, and height values of the three-dimensional model corresponding to the earthen hill space for the outdoor wind field calculation.

(4) CFD Simulation Settings

PHOENICS is the world's first commercial software package for calculating fluid and heat transfer, and it is increasingly being used by researchers to simulate wind environments in residential areas, school campuses, and landscaped gardens. Other software packages for CFD simulation include ANSYS FLUENT v.2019, ENVI-met v.2021, Airpak v.2016, and Butterfly v.2018. PHOENICS-based v.2016 CFD simulation has demonstrated that the height distribution of buildings can have an effect on wind speed and pressure [21] and that adjustments to the building layout can be a viable way to reduce energy consumption and carbon emissions in a community [22]. Moreover, it has been established that the layout of courtyards can have a considerable impact on the outdoor microclimate and the wind and heat comfort of residents [23] and that changes to the building's spatial layout and aspect ratio can create effective ecological buffer spaces [24]. Therefore, PHOENICS is suitable for simulating the wind environment of the earthen hill space in this study. The process of setting up a CFD simulation and establishing the model is outlined below.

Model Selection: Utilizing the RNG k-ε turbulence model from PHOENICS, Equations (4) and (5) are the equations employed. Turbulence modeling can be simulated with the PRESTOL discrete equation and PARSOL function settings. To enhance the accuracy of the computation, small-scale network settings should be applied. PHOENICS also has an automatic convergence detection feature that guarantees reasonable convergence of the results with a precision of 10^{-5} [25].

$$\frac{\partial(\rho k)}{\partial t} + \frac{\partial(\rho k u_i)}{\partial x_i} = \frac{\partial}{x_j}\left(\alpha_k \eta_{eff} \frac{\partial k}{\partial x_j}\right) + G_k + \rho\varepsilon \tag{4}$$

$$\frac{\partial(\rho\varepsilon)}{\partial t} + \frac{\partial(\rho\varepsilon v_i)}{\partial x_i} = \frac{\partial}{\partial x_j}\left(\alpha_\varepsilon \eta_{\Delta f} \frac{\partial\varepsilon}{\partial x_j}\right) + \frac{C_{1s}^{*}\varepsilon}{k} G_k - C_{2s}\rho\frac{\varepsilon^2}{k} \tag{5}$$

In the equations, turbulent kinetic energy is denoted by k, and the turbulent dissipation rate is denoted by ε.

Grid Settings: The computational domain grid is divided into a central region and an edge region (Figure 5c). In the central region, the grid has a planar density of 4 m × 4 m

and a vertical density of 0.5 m. As for the edge region, the grid has a planar density of 8 m × 8 m and a vertical density of 1 m. This grid setting serves to improve the accuracy of the simulation and reduce the number of grid segments, thus increasing the time efficiency. According to the applicable literature [4,5], the computational domain is five times longer and wider than the relevant scene model and three times higher.

Wind Conditions Settings: According to the "Code for Design of Heating, Ventilation and Air Conditioning in Civil Buildings" (GB5073602012, China) [26], the China Weather Network, the China Meteorological Network, and the China Meteorological Data Network, the average summer wind speed in Beijing is 1.9 m/s, with the seasonal dominant wind direction in the southeast direction, and this was used as the inflow boundary condition, with an iteration number of 2000. The chosen ground roughness was 0.2.

3. Results and Discussion

3.1. Comparative Analysis of Measured and Simulated Values

As shown in Table 3 and Figure 6a, the R2 value of 0.804 indicates that 80.4% of the measured wind speed variation can be explained by the simulated wind speed. The linear relationship between the simulated and measured data is strong, indicating a good fit between the PHOENICS-simulated wind speed values and the on-site measured wind speed values. The linear regression equation is $Y = 0.731X - 0.345$. According to Table 4, the *p*-value is less than 0.05, indicating that the linear regression shows significant characteristics. Furthermore, the residuals follow a normal distribution (Figure 6b), suggesting a well-constructed model. This suggests that PHOENICS is suitable for simulating wind environments in hilly spaces and further confirms the validity of CFD simulation data for 42 hilly spatial enclosure layouts.

Table 3. Model summary [b].

Model	R	R Squared	Adjusted R Squared	Std. Error of the Estimate	Durbin–Watson
1	0.896 [a]	0.804	0.776	0.09391	0.824

[a]. Predictors (constant): simulated wind speed. [b]. Dependent variable: measured wind speed.

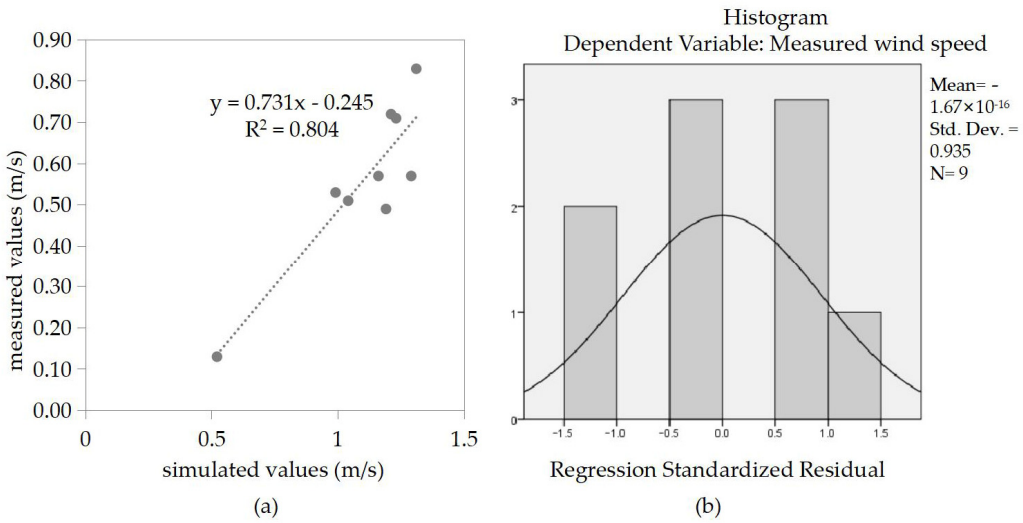

Figure 6. (**a**) Linear regression plot of measured and CFD-simulated values. (**b**) Histogram of the regression standardized residual.

Table 4. ANOVA [a].

Model		Sum of Squares	df	Mean Squared	F	Sig.
1	Regression	0.253	1	0.253	28.647	0.001 b
	Residual	0.062	7	0.009		
	Total	0.314	8			

[a]. Dependent variable: measured wind speed. [b]. Predictors (constant): simulated wind speed.

3.2. Influence of the Enclosure Layout Index in Earthen Hill Space on the Wind Environment

PHOENICS was utilized to assess the influence of the enclosure layout of earthen hills in terms of spatial directions, densities, and area indices on the wind environment for 42 earthen hill spatial models of the Old Summer Palace Ruins Park. The wind speed and wind pressure at a height of 1.5 m (Z = 1.5 m) from the ground for pedestrians were obtained from the CFD simulations (Tables 5 and 6 and Figures 7 and 8).

Table 5. Statistical values of summer wind speed in 42 earthen hill spaces of the Old Summer Palace Ruins Park.

Figure No.	Direction Index	Density Index	Area Index	Detection Points of Wind Speed (m/s)									D-Value
				A	B	C	D	E	F	G	H	I	
1	4	0.886	1.34	1.30	1.43	1.39	1.49	1.51	1.48	1.41	1.51	0.21	1.34
2	1	0.351	1.48	1.53	1.59	1.59	1.57	1.59	1.58	1.45	1.58	0.14	1.48
3	3	0.482	1.45	1.53	1.47	1.58	1.57	1.58	1.53	1.48	1.57	0.13	1.45
4	2	0.128	1.59	1.59	1.57	1.52	1.54	1.50	1.42	1.51	1.56	0.17	1.59
5	3	0.452	1.34	1.29	1.09	-	1.60	1.60	1.71	1.27	1.59	0.62	1.34
6	2	0.288	1.55	1.53	1.55	-	-	-	0.00	1.38	1.53	1.55	1.55
7	4	0.957	1.48	1.51	1.48	1.34	1.30	1.18	1.35	1.41	1.50	0.33	1.48
8	3	0.410	1.40	1.46	-	-	1.59	1.30	1.39	1.48	-	0.29	1.40
9	4	0.895	1.56	1.48	1.39	1.49	1.52	1.50	1.34	0.00	1.52	1.56	1.56
10	4	0.781	1.43	1.51	1.41	1.19	0.62	1.36	1.49	1.24	1.39	0.88	1.43
11	2	0.388	1.58	1.69	1.25	0.97	1.54	1.56	1.57	1.48	1.55	0.72	1.58
12	2	0.389	1.59	1.62	1.69	1.48	1.58	1.00	1.36	1.44	1.58	0.70	1.59
13	4	0.953	1.57	0.95	1.02	1.22	-	1.15	1.18	1.41	1.46	0.63	1.57
14	3	0.758	1.51	1.49	1.36	1.40	0.80	1.41	0.00	1.12	1.49	1.51	1.51
15	1	0.211	1.60	1.58	1.29	1.50	1.56	1.57	1.57	1.59	1.57	0.31	1.60
16	4	0.893	0.77	1.23	1.43	1.51	1.53	0.41	1.38	1.44	1.51	1.12	0.77
17	2	0.606	1.49	1.56	1.59	1.55	1.30	0.77	1.42	1.49	1.55	0.82	1.49
18	2	0.391	1.59	1.32	1.45	1.60	1.59	1.60	1.69	1.52	1.60	0.37	1.59
19	1	0.140	1.63	1.62	1.58	1.58	1.57	1.57	1.62	1.63	1.62	0.06	1.63
20	2	0.615	1.51	1.55	1.57	1.57	1.56	1.53	0.00	0.00	1.54	1.57	1.51
21	3	0.617	1.50	1.50	1.60	1.53	1.53	1.51	1.49	1.44	1.51	0.16	1.50
22	1	0.119	1.59	1.58	1.59	1.55	1.53	1.56	1.55	1.56	1.58	0.06	1.59
23	4	0.761	1.37	1.28	0.00	1.39	1.35	1.53	0.00	1.37	1.52	1.53	1.37
24	3	0.563	1.56	1.45	1.42	1.56	1.57	1.57	1.28	1.49	1.57	0.29	1.56
25	2	0.284	1.47	1.41	1.57	1.54	1.41	-	1.55	1.50	1.56	0.16	1.47
26	1	0.210	1.63	1.62	1.45	1.53	1.56	1.58	1.58	1.59	1.59	0.19	1.63
27	1	0.405	1.56	0.00	1.63	1.50	1.47	0.00	1.41	1.55	0.00	1.63	1.56
28	3	0.419	1.41	1.53	1.54	1.53	1.53	1.53	1.52	1.50	1.53	0.13	1.41
29	2	0.478	1.64	-	1.63	1.52	1.35	1.23	1.35	1.50	1.57	0.41	1.64
30	2	0.262	1.54	1.63	1.51	1.39	1.43	-	1.20	1.46	1.48	0.44	1.54
31	4	0.835	1.19	0.97	1.32	1.41	0.98	1.10	0.00	1.12	-	1.41	1.19
32	3	0.471	1.58	-	-	-	1.60	1.08	1.40	1.60	-	0.52	1.58
33	2	0.519	1.59	-	-	-	-	1.14	0.84	0.00	-	1.59	1.59
34	3	0.186	1.10	1.44	1.58	-	1.51	-	1.61	1.49	-	0.52	1.10
35	2	0.516	0.71	0.00	1.57	-	-	-	1.27	1.24	-	1.57	0.71
36	2	0.264	1.61	1.67	0.00	1.56	1.61	1.62	1.59	1.51	1.61	1.67	1.61
37	1	0.301	0.00	0.00	1.68	1.62	1.50	1.52	1.45	1.49	1.52	1.68	0.00
38	4	0.981	1.51	1.47	1.43	1.16	0.95	0.96	0.00	1.27	1.52	1.52	1.51
39	3	0.675	1.44	1.44	1.32	-	1.12	0.00	1.56	1.47	1.35	1.56	1.44
40	2	0.535	1.46	1.34	1.48	1.30	1.39	-	-	-	1.53	0.23	1.46
41	3	0.548	-	-	1.37	1.35	1.21	1.12	1.34	-	1.51	0.39	-
42	3	0.607	0.50	0.63	0.99	1.26	1.46	1.63	0.88	0.44	0.98	1.18	0.50

Note: The red color indicates the greatest wind speed and wind difference at each detection point in the 42 earthen hill spaces, the green color denotes the least wind speed and wind difference at each detection point, the blue color signifies detection points with wind speeds below 1 m/s (in this case, the lowest wind speed detection points will no longer be shown in green), and the light gray background illustrates spaces with uncomfortable wind speed detection points.

Table 6. Statistical values of summer wind pressure difference in 42 earthen hill spaces of the Old Summer Palace Ruins Park.

Figure No.	Direction Index	Density Index	Area Index	Maximum Wind Pressure Difference	Figure No.	Direction Index	Density Index	Area Index	Maximum Wind Pressure Difference
1	4	0.886	1.034	1.658	22	1	0.119	14.406	0.318
2	1	0.351	2.914	1.367	23	4	0.761	1.241	1.443
3	3	0.482	3.174	1.135	24	3	0.563	2.967	1.251
4	2	0.128	42.291	0.483	25	2	0.284	6.155	0.735
5	3	0.452	1.710	1.48	26	1	0.21	8.120	0.509
6	2	0.288	6.573	1.419	27	1	0.405	1.134	1.427
7	4	0.957	0.880	1.287	28	3	0.419	2.907	1.393
8	3	0.41	0.415	1.352	29	2	0.478	2.514	1.248
9	4	0.895	0.579	1.478	30	2	0.262	0.306	1.465
10	4	0.781	0.694	1.408	31	4	0.835	0.782	1.494
11	2	0.388	4.566	1.493	32	3	0.471	0.271	1.889
12	2	0.389	5.608	1.212	33	2	0.519	0.378	1.906
13	4	0.953	0.833	1.512	34	3	0.186	0.617	1.453
14	3	0.758	0.613	0.977	35	2	0.516	0.476	1.472
15	1	0.211	5.111	0.931	36	2	0.264	1.714	1.401
16	4	0.893	1.454	1.329	37	1	0.301	1.021	1.814
17	2	0.606	0.700	1.556	38	4	0.981	0.637	2.077
18	2	0.391	2.772	1.566	39	3	0.675	0.250	1.032
19	1	0.14	9.434	0.818	40	2	0.535	0.435	1.254
20	2	0.615	2.036	1.119	41	3	0.548	0.432	2.029
21	3	0.617	1.272	0.798	42	3	0.607	0.751	1.946

Note: The red highlighting indicates the greatest wind pressure difference among the 42 earthen hill spaces, while the green highlighting denotes the least wind pressure difference. The light gray shading indicates earthen hill spaces with wind pressure differences below 0.5 Pa.

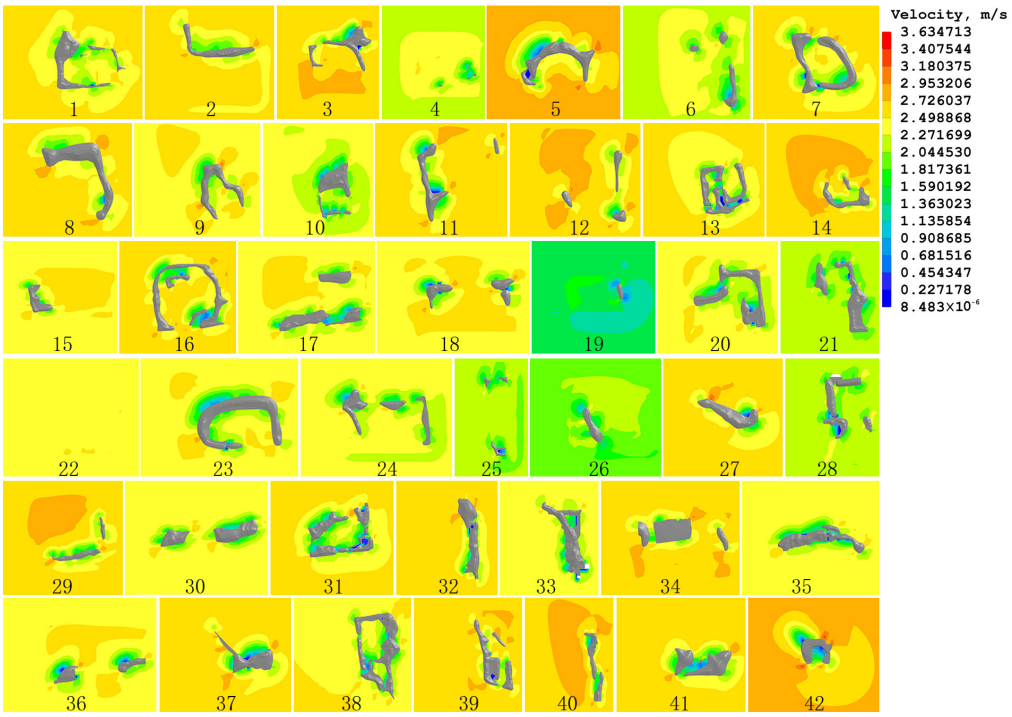

Figure 7. Wind speed map of 42 earthen hill spaces in the Old Summer Palace Ruins Park in summer.

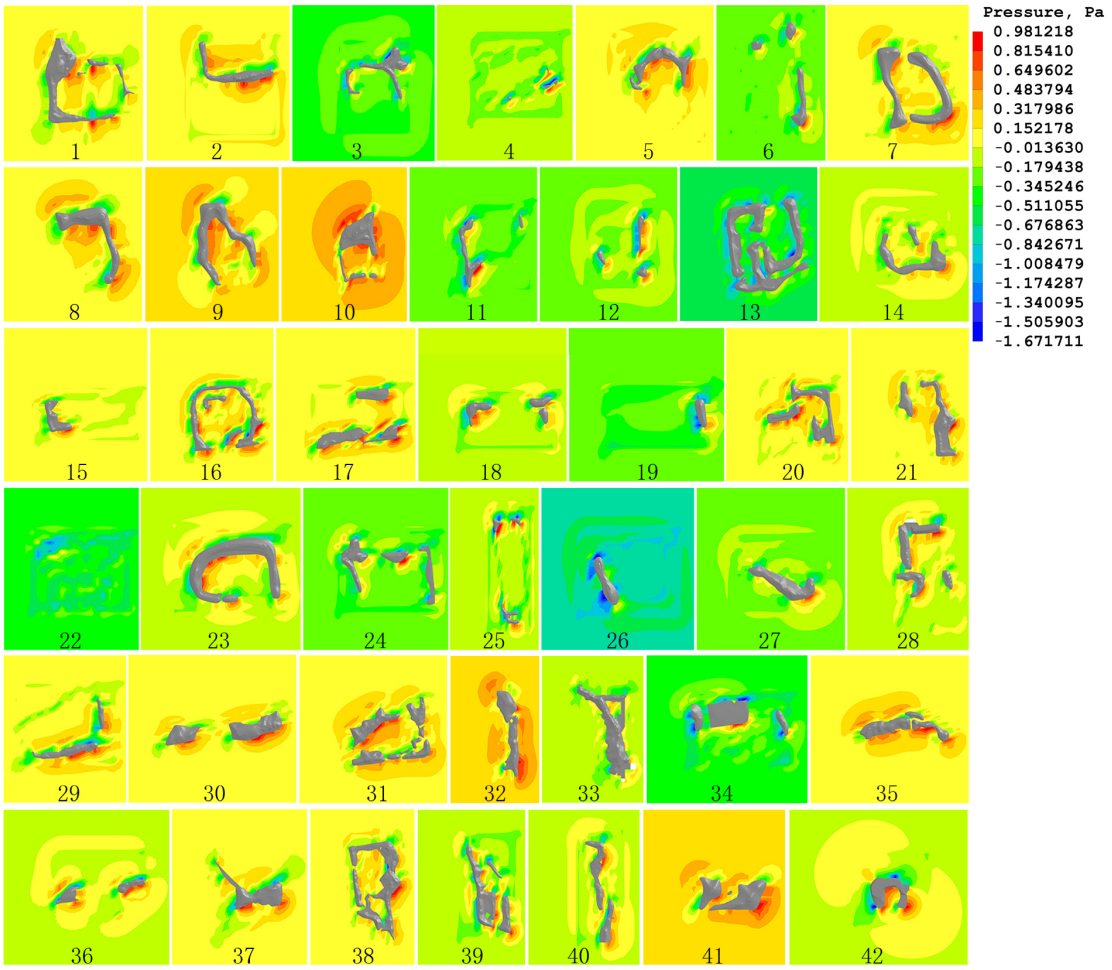

Figure 8. Wind pressure distribution for 42 earthen hill spaces in the Old Summer Palace Ruins Park in summer.

3.2.1. Influence of Directional Index on Wind Environment

Analysis of Table 5 and Figure 7 reveals that the average summer wind speed of the 42 earthen hill spaces in the Old Summer Palace Ruins Park is between 0 and 1.71 m/s, with no powerful gusts. Out of the total 378 wind speed detection points in the 42 earthen hill spaces, 90.74% of the wind speeds measured fall between 1 and 2.9 m/s, while the remaining 9.26% are less than 1 m/s, suggesting the occurrence of certain still winds in the summer season. In terms of orientation index classification, statistical analysis was conducted on the number of earthen hill spaces containing uncomfortable wind speed detection points in 42 independent spaces based on the enclosure layout direction classification (Figure 9a). The results show that in summer, the majority of earthen hill spaces containing uncomfortable wind speed detection points were in those with direction index 4, followed by direction index 2, 1, and 3. The earthen hill space with three direction layouts had the best wind comfort. As the direction index of the enclosure layout in the earthen hill space increased, the sense of enclosure also increased, resulting in fluctuating changes in wind comfort, with an overall upward trend of discomfort. In summer, the interiors of earthen hill spaces are more likely to suffer from poor air circulation and long-term accumulation of pollutants.

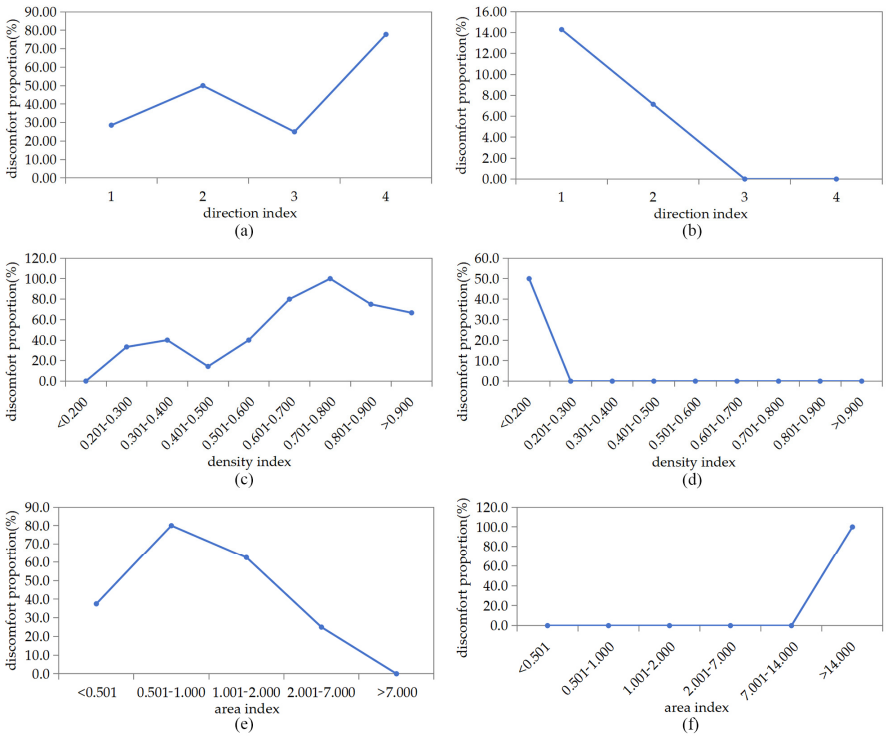

Figure 9. (**a**) Comparison of the number of spaces with uncomfortable wind speed detection points among 42 earthen hill spaces classified according to the enclosure layout direction. (**b**) Comparison of the number of spaces with wind pressure differences less than 0.5 Pa among 42 earthen hill spaces classified according to the direction of the enclosure layout. (**c**) Comparison of the number of spaces with uncomfortable wind speed detection points among 42 earthen hill spaces classified according to the enclosure layout density. (**d**) Comparison of the number of spaces with wind pressure differences less than 0.5 Pa among 42 earthen hill spaces classified according to the density of the enclosure layout. (**e**) Comparison of the number of spaces with uncomfortable wind speed detection points among 42 earthen hill spaces classified according to the enclosure layout area. (**f**) Comparison of the number of earthen hill spaces with wind pressure differences less than 0.5 Pa among 42 earthen hill spaces classified according to the area of the enclosure layout.

In terms of wind pressure, as shown in Table 6 and Figure 8, the analysis of wind pressure in the 42 earthen hill spaces of the Old Summer Palace Ruins Park during summer revealed a maximum wind pressure difference of 2.077 Pa and a minimum wind pressure difference of 0.318 Pa. A total of 95.24% of the earthen hill spaces had a wind pressure difference greater than 0.5 Pa, indicating that the summer ventilation is generally favorable. However, the 4th and 22nd earthen hill spaces had a wind pressure difference lower than 0.5 Pa, making them unsuitable for ventilation. Additionally, the wind pressure difference in the earthen hill space increased as the spatial direction index increased, with the maximum pressure difference on No. 38 (direction index 4) and the minimum wind pressure difference on No. 22 (direction index 1). In terms of orientation index classification, a statistical analysis was conducted on the number of spaces with wind pressure differences below 0.5 Pa out of 42 earthen hill spaces according to the enclosure layout direction classification (Figure 9b). As the direction index of the enclosure layout of the earthen hill space increases, the likelihood of wind pressure differences below 0.5 Pa decreases, making summer ventilation more favorable.

It is evident that the enclosure layout of the earthen hill space with a higher direction index results in a lower wind speed and a greater chance of experiencing calm winds. The three-element layout, a type of enclosure layout, offers a high sense of enclosure, optimal wind comfort, and better ventilation.

3.2.2. Influence of Density Index on Wind Environment

In terms of wind speed, statistical analysis was carried out on the number of spaces that contained uncomfortable wind speed detection points in 42 independent earthen hill spaces based on the density classification of the enclosure layout (Figure 9c). During the summer months, the presence of uncomfortable wind speed detection points in 42 independent earthen hill spaces varied in accordance with the density index. When the density index was lower than 0.200, no uncomfortable wind speed detection points were observed; however, when the density index was higher than 0.200, the optimal wind-comfortable earthen hill space had a density index between 0.401 and 0.500, while the worst was between 0.701 and 0.800. With a higher density index of the enclosure layout in the earthen hill space, the fullness and squareness of the space increase, and the wind comfort fluctuates, leading to an overall increase in discomfort.

In terms of wind pressure, statistical analysis was conducted on the number of spaces with a wind pressure difference of less than 0.5 Pa out of 42 earthen hill spaces (Figure 9d) based on the enclosure layout's density classification in order to assess the wind pressure. As the density index of the enclosure layout in the earthen hill spaces grew, the instances of wind pressure differences below 0.5 Pa decreased. When the density index was higher than 0.200, there were no longer any wind pressure differences of less than 0.5 Pa, which was beneficial for summer ventilation.

The above analysis indicates that as the density index of the enclosure layout in the earthen hill space increases, the wind speed decreases, and the likelihood of experiencing calm winds increases. An earthen hill space with a density index between 0.401 and 0.500 is a type of enclosure layout that combines the fullness and squareness of the space, the highest level of wind comfort, and improved ventilation.

3.2.3. Influence of Area Index on Wind Environment

In terms of wind speed, statistical analysis was conducted on the number of spaces containing uncomfortable wind speed detection points among 42 independent earthen hill spaces based on the area classification of the enclosure layout (Figure 9e). As the area index increases, the number of soil mountain spaces with uncomfortable wind speed detection points in the 42 independent earthen hill spaces in summer fluctuates with a peak pattern. The area index ranges from 0.501 to 1.000, with the worst wind comfort. When the area index is greater than 7.000, the wind comfort improves. The area indices of the enclosure layout in the earthen hill space increase, leading to an increase in the sense of the outdoor activity scale within the earthen hill space, resulting in a peak change in its wind comfort; however, in the long run, the discomfort is seen to decrease.

In terms of wind pressure, an analysis of the statistical data for the 42 earthen hill spaces was conducted to determine the number of instances in which the wind pressure differences were below 0.5 Pa, based on the enclosure layout area classification (Figure 9f). With the increase in the area index of the enclosure layout of the earthen hill, there is a situation where the wind pressure difference is less than 0.5 Pa. Only when the area index is greater than 7.000 does a situation develop in which the wind pressure difference is less than 0.5 Pa, which is not conducive to summer ventilation.

It is evident that the area index of the enclosure layout in the earthen hill space has an influence on the wind speed: the higher the area index, the higher the wind speed and the lower the probability of having calmer winds. This layout, with an area index between 7.001 and 14.000, offers the optimum combination of outdoor activity, wind comfort, and ventilation in an earthen hill space.

4. Conclusions

In this study, we focused on the enclosure layout of the Old Summer Palace Ruins Park in Beijing. We established 42 independent earthen hill spatial models to investigate the effects of direction, density, and area on the spatial wind environment of an earthen hill. Formulas for the direction index, density index, and area index of the earthen hill's

enclosure layout were constructed, and the corresponding values of the 42 earthen hill spaces were statistically analyzed. We determined the evaluation criteria for the summer monsoon environment in the earthen hill space. Using a validated CFD simulation model, the summer wind speed and pressure values for the 42 earthen hill spaces were obtained, and a comparative analysis was conducted from three aspects: direction, density, and area index. We concluded that the spatial wind environment of the earthen hill is impacted by direction, density, and area. The results of the study are as follows:

(1) After comparing the direction index, it was discovered that higher direction indices were associated with lower wind speeds, calm winds, and better ventilation. Based on this information, a direction index of 3 was determined to be the best option for the enclosure layout of the earthen hill space; this choice provides a high sense of enclosure, great wind comfort, and remarkable wind permeability.

(2) After analyzing the wind environment of an earthen hill space, it was found that the density index has a significant impact on wind speed, calmness of the wind, and ventilation. A higher density index leads to lower wind speed and a greater likelihood of calm winds, resulting in better ventilation. It was concluded that the optimal density index for the enclosure layout of an earthen hill space is between 0.401 and 0.500. This range offers a combination of high fullness, squareness, excellent wind comfort, and high wind permeability.

(3) An examination was carried out of the wind environment in earthen hill spaces with regard to the area index. The results show that as the area index increases, the wind speed also increases, the chances of still air decrease, and the ventilation becomes poorer. Earthen hill spaces with an area index ranging from 7.001 to 14.000 are most suitable for the enclosure layout of earthen hill spaces, offering ample outdoor activity areas, optimal wind comfort, and excellent wind permeability.

(4) We examined the influence of three plane indices (direction, density, and area) on the internal wind environment of the enclosure layout of an earthen hill. The results suggest that the selection of direction, density, and area indices can optimize the wind comfort in the earthen hill space, confirming the advantages of the enclosure layout in an earthen hill and reflecting the ecological wisdom of that layout in ancient China.

In the future, we will perform a comparative analysis of the effects of façade indices, such as aspect ratio, permeability, and saturation, on the wind environment of the enclosure layout of earthen hill spaces. To avoid the risk of excessive length and unrelated topics, this analysis will be performed separately. New technologies can also be used to scientifically verify the various construction practices accumulated in the long-term development of traditional Chinese gardens.

Author Contributions: Conceptualization, Z.W. and M.W.; methodology, Y.W. and T.H.; software, T.H. and J.C.; validation, Z.W., T.L., M.W. and J.C.; formal analysis, Z.W., T.L. and M.W.; investigation, Z.W. and Y.W.; resources, Z.W.; data curation, Z.W. and J.C.; writing—original draft preparation, Z.W. and M.W.; writing—review and editing, Z.W., T.L. and J.C.; visualization, J.C.; supervision, T.L., T.H. and J.C.; project administration, Z.W.; funding acquisition, Z.W. All authors have read and agreed to the published version of the manuscript.

Funding: This work was supported by the Ministry of Education, Humanities, and Social Science research youth fund projects [20YJCZH009]; the research project of the Southeast Ecological Vulnerable Zone Detection and Restoration Engineering Technology Innovation Center of the Ministry of Natural Resources [KY03000000402023017]; the Fujian young and middle-aged teacher education research projects [JAT210303]; the key research funds for Fujian Province public-interest scientific institution in China [2020R1002006]; and the general project for Fujian Province natural science foundation in China [2023J01894].

Institutional Review Board Statement: Not applicable.

Informed Consent Statement: Not applicable.

Data Availability Statement: Data is contained within the article.

Conflicts of Interest: The authors declare no conflicts of interest.

References

1. Chen, X.; Sun, X. Study on Mountain Confucian Temple Spatial Layout and Landscape Environment: An Analytical Study of Confucian Temples in Southwest China during the 15th–19th Centuries. *J. Asian Archit. Build. Eng.* **2023**, *22*, 1–17.
2. Cheng, J. *Feng Shui and Architecture*; Central Compilation and Translation Press: Beijing, China, 2016; p. 42.
3. Tang, L.; Nikolopoulou, M.; Zhao, F.; Zhang, N. CFD modeling of the built environment in Chinese historic settlements. *Energy Build.* **2012**, *55*, 601–606. [CrossRef]
4. Zhao, Z.; Zhang, S.; Peng, Y. Analysis of Winter Environment Based on CFD Simulation: A Case Study of Long–Hu Sand Feng Shui Layout at Jiangxi Bailudong Academy Complex. *Buildings* **2023**, *13*, 1101. [CrossRef]
5. Guo, P.; Ding, C.; Guo, Z.; Liu, T.; Lyu, T. Coupling CFD Simulation and Field Experiments in Summer to Prove Feng Shui Optimizes Courtyard Wind Environments: A Case Study of Prince Kung's Mansion in Beijing. *Buildings* **2022**, *12*, 629. [CrossRef]
6. Wang, K.; Liang, H.; Yan, Y. Wind field law of different terrain patterns based on computational fluid dynamics simulation and application in wind sensing planning. *Acta Ecol. Sin.* **2021**, *41*, 3499–3511.
7. Zhou, Z.; Deng, J.; Wang, P.; Zhou, C.; Xu, Y.; Jiang, W.; Ma, K. Physical Environment Study of Traditional Village Patterns in Jinxi County, Jiangxi Province Based on CFD Simulation. *Processes* **2022**, *10*, 2453. [CrossRef]
8. Xiong, Y.; Zhang, J.; Yan, Y.; Sun, S.; Xu, X.; Higueras, E. Effect of the spatial form of Jiangnan traditional villages on microclimate and human comfort. *Sustain. Cities Soc.* **2022**, *87*, 104136. [CrossRef]
9. Wang, Z.; Wang, Y.; Wu, G.; Lu, T. Simulation analysis of wind environment in traditional villages under natural ven-tilation conditions: An example of Quanfang village in Jinxi County. *Urban Archit.* **2022**, *19*, 20–22.
10. Ai, Z.T.; Mak, C.M. CFD simulation of flow in a long street canyon under a perpendicular wind direction: Evaluation of three computational settings. *Build. Environ.* **2017**, *114*, 293–306. [CrossRef]
11. Gan, S.; Li, G.; Li, H. Assessment of wind energy potential within through-building openings under twisted wind flows. *Build. Nvironment* **2023**, *244*, 110773. [CrossRef]
12. Almhafdy, A.; Ibrahim, N.; Ahmad, S.S.; Yahya, J. Thermal Performance Analysis of Courtyards in a Hot Humid Climate Using Computational Fluid Dynamics CFD Method. *Procedia—Soc. Behav. Sci.* **2015**, *170*, 474–483. [CrossRef]
13. Villagrán, E.; Flores-Velazquez, J.; Akrami, M.; Bojacá, C. Influence of the Height in a Colombian Multi-Tunnel Greenhouse on Natural Ventilation and Thermal Behavior: Modeling Approach. *Sustainability* **2021**, *13*, 13631. [CrossRef]
14. Hong, B.; Qin, H.; Jiang, R.; Xu, M.; Niu, J. How Outdoor Trees Affect Indoor Particulate Matter Dispersion: CFD Simulations in a Naturally Ventilated Auditorium. *Int. J. Environ. Res. Public Health* **2018**, *15*, 2862. [CrossRef] [PubMed]
15. Zhao, Y.; Chen, Y.; Li, K. A simulation study on the effects of tree height variations on the facade temperature of enclosed courtyard in North China. *Build. Environ.* **2022**, *207 Pt B*, 108566. [CrossRef]
16. Zhou, W. *History of Chinese Classical Gardens*, 2nd ed.; Tsinghua University Press: Beijing, China, 1999; p. 517.
17. *GB/T 50378-2019*; Green Building Evaluation Standard. China Construction Industry Press: Beijing, China, 2019; pp. 126–127.
18. Murakami, S.; Morikawa, Y. Creteria For Assessing Wind-Induced Discomfort Considering Temperature Effect. *J. Archit. Plan. Environ. Eng.* **1985**, *358*, 9–17.
19. Zhang, H. Research on Natural Ventilation Design of Rural Housing in Yangtze River Delta. Ph.D. Thesis, Southeast University, Nanjing, China, 2016.
20. Tan, L. *Simulation Study on Outdoor Wind Environment in Residential Areas Based on Reasonable Quiet Wind Rate Determination*; Chongqing University: Chongqing, China, 2017.
21. Lu, M.; Song, D.; Shi, D.; Liu, J.; Wang, L. Effect of High-Rise Residential Building Layout on the Spatial Vertical Wind Environment in Harbin, China. *Buildings* **2022**, *12*, 705. [CrossRef]
22. Xuan, W. Research on Reducing Carbon Consumption in Residential Community Spaces as Influenced by Microclimate Environments. *J. Urban Plan. Dev.* **2021**, *9*, 147.
23. Li, J.; Liu, J.; Srebric, J.; Hu, Y.; Liu, M.; Su, L.; Wang, S. The Effect of Tree-Planting Patterns on the Microclimate within a Courtyard. *Sustainability* **2019**, *11*, 1665. [CrossRef]
24. Xu, X.; Luo, F.; Wang, W.; Hong, T.; Fu, X. Performance-Based Evaluation of Courtyard Design in China's Cold-Winter HotSummer Climate Regions. *Sustainability* **2018**, *10*, 3950. [CrossRef]
25. Chu, C.-R.; Su, Z.-Y. Natural Ventilation Design for Underground Parking Garages. *Build. Environ.* **2023**, *227*, 109784. [CrossRef]
26. *GB50736-2012*; Code for Design of Heating, Ventilation and Air Conditioning in Civil Buildings. China Construction Industry Press: Beijing, China, 2012; pp. 47–50.